Computerized Medical Imaging and Graphics 103 (2023) 102140

Contents lists available at ScienceDirect

Computerized Medical Imaging and Graphics

journal homepage: www.elsevier.com/locate/compmedimag

Template-based graph registration network for boosting the diagnosis of brain connectivity disorders

Zeynep Gürler [a], Mohammed Amine Gharsallaoui [a,b], Islem Rekik [a,c,1,*], for the Alzheimer's Disease Neuroimaging Initiative

[a] BASIRA lab, Faculty of Computer and Informatics, Istanbul Technical University, Istanbul, Turkey
[b] Ecole Polytechnique de Tunisie, Tunisia
[c] Computing, Imperial-X Translation and Innovation Hub, Imperial College London, London, UK

ARTICLE INFO

Keywords:
Brain graph registration
Graph neural networks
Connectional brain template
Adversarial learning
Brain dysconnectivity disorder diagnosis

ABSTRACT

Brain graphs are powerful representations to explore the biological roadmaps of the human brain in its healthy and disordered states. Recently, a few graph neural networks (GNNs) have been designed for brain connectivity synthesis and diagnosis. However, such non-Euclidean deep learning architectures might fail to capture the neural interactions between different brain regions as they are trained without guidance from any prior biological template—i.e., *template-free learning*. Here we assume that using a population-driven brain connectional template (CBT) that captures well the connectivity patterns fingerprinting a given brain state (e.g., healthy) can better guide the GNN training in its downstream learning task such as classification or regression. To this aim we design a plug-in *graph registration network* (GRN) that can be coupled with any conventional graph neural network (GNN) so as to boost its learning accuracy and generalizability to unseen samples. Our GRN is a graph generative adversarial network (gGAN), which registers brain graphs to a *prior* CBT. Next, the registered brain graphs are used to train typical GNN models. Our GRN can be integrated into any GNN working in an end-to-end fashion to boost its prediction accuracy. Our experiments showed that GRN remarkably boosted the prediction accuracy of four conventional GNN models across four neurological datasets.

1. Introduction

Deep Learning (DL) has dominated the research field of clinical decision making including brain disease diagnosis (Suzuki, 2017; Lee et al., 2017). Recent works (Asiri et al., 2019) designing computer-aided diagnosis (CAD) systems have integrated DL diagnosis models to be more robust and powerful in discriminating between disordered and healthy patients. DL has an outstanding ability to learn multi-level representation of medical imaging data such as Magnetic Resonance Imaging (MRI) or resting-state functional MRI (rs-fMRI) (Suzuki, 2017; Lee et al., 2017). Such non-invasive imaging technologies provide anatomical features such as gray matter volumes and cortical thickness as potential clinical biomarkers of particular neurological disorders—to mention just a few. However, the brain is a compound, highly and internally connected system. Thus, such simple features might fail to capture the brain interconnectedness (van den Heuvel and Sporns, 2019; Fornito et al., 2015). Thanks to their ability to represent connections between different entities, graphs are powerful representations to exhibit the relational information between different anatomical regions of interest (ROIs) in the brain.

Several studies on brain graph analysis focused on node classification, link prediction, and graph classification using particular machine learning (ML) methods (Richiardi et al., 2013; Du et al., 2018). For instance, Khazaee et al. (2015) constructed connectivity matrices derived from rs-fMRI data and performed statistical analysis using ANOVA and forward sequential feature selection to obtain discriminative feature vectors. Next, they trained a support vector machine (SVM) classifier based on these discriminative feature vectors to distinguish between Alzheimer's (AD), Mild Cognitive Impairment (MCI), and healthy patients. A very recent paper (Bilgen et al., 2020) examined a diverse pool of machine learning pipelines in classifying cortical brain networks. Nonetheless, traditional ML methods merely work for a specific task or a dataset and rarely generalize to other datasets and tasks which indicates that they lack the ability of generalizability. Therefore, Graph Neural Networks (GNN) come forward with their higher

* Corresponding author at: BASIRA lab, Faculty of Computer and Informatics, Istanbul Technical University, Istanbul, Turkey.
E-mail address: i.rekik@imperial.ac.uk (I. Rekik).
URL: http://basira-lab.com/ (I. Rekik).
[1] GitHub code:https://github.com/basiralab/GRN.

https://doi.org/10.1016/j.compmedimag.2022.102140
Received 9 April 2022; Received in revised form 11 October 2022; Accepted 2 November 2022
Available online 19 November 2022

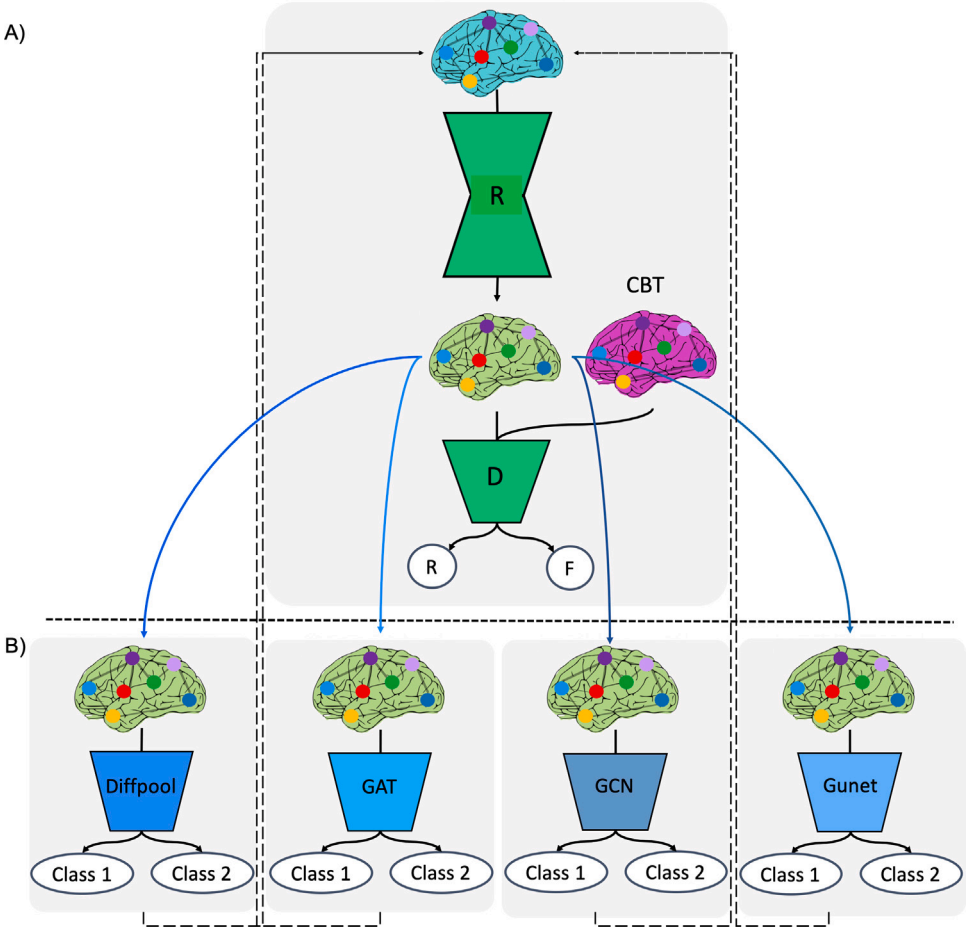

Fig. 1. *Illustration of classification network concept* (A) Our graph registration framework registers input brain graphs to a prior connectional brain template (CBT). (B) We input the registered brain graphs to conventional graph neural networks for classification. Our model is trained in an end-to-end fashion and back-propagates through the whole network. R: registration network. D: discriminator network.

generalizability to non-Euclidean data and powerful performance. However, there are very limited works on Graph Neural Networks (GNNs) for brain graph classification as reported in a recent review paper (Bessadok et al., 2022).

For graph classification and graph representation, Geometric Deep Learning (GDL) has become a leading focal point in various areas such as social science (Hamilton et al., 2018), e-commerce networks (Li et al., 2020), natural science (biology networks) (Bove et al., 2020), and traffic networks (Diehl et al., 2019; Mallick et al., 2020). GNNs root in several fundamental concepts (Zhou et al., 2018), which are Convolutional Neural Networks (CNNs) and graph embedding—to mention just a few. CNNs with multi-layer architectures extract high-order representations from raw input data to map them into the desired output. The multi-layer architecture helps attain valuable information from hierarchical patterns, which refer to non-Euclidean data of graphs. Also, CNNs acknowledge regional connections in images, which are the fundamental data source of CNNs, by reconstructing their localized spatial features. Therefore, CNN is a strong concept to adapt for GNNs. Accordingly, Kipf and Welling (2017) proposed Graph Convolutional Network (GCN), which applies convolutional operations to graphs to learn a hidden layer that captures both local graph structures and node features and scales the graph edges to a desired output feature map. Another work (Veličković et al., 2018) introduced Graph Attentional Network (GAT), an attention-based architecture that generates hidden representations for each node in a graph by calculating the importance of each neighbor. These GNN methods reproduce features from the graph edges linearly and overlook to learn the hierarchical representations of graphs, which might be questionable over the graph classification task where the aim is to try to predict the label of an entire graph. To overcome this limitation, Ying et al. (2019) proposed DiffPool, a differentiable graph pooling module for hierarchical graph representation. DiffPool embeds graphs using GNNs and clusters these embeddings as nodes to generate a new graph at each hierarchical layer. The number of layers is a hyperparameter and the last layer outputs the classified label. Lastly, Gao and Ji (2019) came up with an encoder–decoder architecture for graphs and introduced graph U-Nets (g-U-Nets), which consists of graph pooling (gPool) and graph un-pooling (gUnpool) blocks.

Although such conventional models deliver powerful performance in several graph applications, they have some limitations when the task domain is *network neuroscience* due to the complexity and richness of brain connectivity graphs (Bessadok et al., 2022). In fact, brain connectomes are biological roadmaps of brain connections between different anatomical ROIs. It is hence crucial to preserve the topological soundness of such biological roadmaps in downstream learning tasks such as brain synthesis, classification or regression (Bessadok et al., 2022). Besides, existing GNN architectures might fail to capture the neural interactions between different brain regions as they are trained without guidance from any prior biological template—i.e., *template-free learning* (Bessadok et al., 2022). The concept of template-based learning is commonly used on Euclidean data such as *images*. In fact, image-based brain atlases or templates are commonly used to register an input image to a prior image-based template (e.g., MRI) for abnormality detection, disorder diagnosis, brain mapping and evolution trajectory prediction—among other purposes (Fan et al., 2006; Davatzikos et al., 2011; Kim et al., 2016; Min et al., 2014; Liu et al., 2015; Gafuroglu

and Rekik, 2019; Li et al., 2019). Simply put, image registration aims to apply a geometric transformation to input images for aligning them onto a fixed prior image. The minimization of the difference between the aligned image and the fixed image template determines the success in image registration. A considerable amount of studies worked on image registration in medical imaging for various tasks (Sokooti et al., 2017; Hu et al., 2018; Balakrishnan et al., 2019; de Vos et al., 2019). However, while there is an abundance of *image-based registration* methods in the neuroscience and neuroimaging literature, *graph-based registration* remains an uncharted territory.

To fill this gap and motivated by the outperformance *template-guided* or *atlas-guided* learning tasks over the template-free methods, we set out to generalize the concept of image registration to graphs and demonstrate its value in boosting classification accuracy of brain states. Here, we assume that using a population-driven brain connectional template (CBT) (Rekik et al., 2017; Dhifallah and Rekik, 2020; Gurbuz and Rekik, 2020; Gürbüz and Rekik, 2021) that captures well the connectivity patterns fingerprinting a given brain state (e.g., healthy) can better guide the GNN training in its downstream learning task such as classification or regression. Specifically, we drive inspiration from the recent works on integrational network neuroscience where CBTs are derived from input brain graph populations (Dhifallah and Rekik, 2020; Gurbuz and Rekik, 2020) and propose a Graph Registration Network (GRN). Our GRN acts as a *plug-in network* that can be coupled with any conventional graph neural network in an end-to-end fashion to boost its learning accuracy and generalizability to unseen samples. Particularly, our GRN is a graph generative adversarial network (gGAN), which registers brain graphs to a *prior* CBT. Training in an end-to-end fashion makes each step act dependently with each other and send feedback to each other, which helps optimize the learning process. Next, the registered brain graphs are used to train typical GNN models.

Fig. 1 illustrates the main concept of our brain graph registration and classification framework. First, we register brain graphs with respect to a *graph-based* template (here CBT) and obtain registered brain graphs that preserve the common interactional neural patterns. Registering the input brain graphs to a prior CBT might help preserve the brain topology and also better bring out the unique features of individual brain graphs. In fact, such graph registration step will enable to tease apart the *individuality* of each brain connectome by simply comparing its registered version with the prior population CBT. The registered brain graphs are then inputted to the conventional GNNs as they better capture the individual traits of their topology for the target learning task (e.g., classification). Below, we articulate the main contributions of our work at different levels:

1. We propose a plug-in network that can eventually work with other GNN architecture and be combined with other downstream learning tasks.
2. We propose a network that works in an end-to-end manner by optimizing a joint loss function of both registration and classification networks at each iteration.
3. Our GRN generalizes the registration concept to graphs to boost the classification performance of any GNN architecture.
4. Our plug-in GRN is a generic model. It can be trained using any type of graph templates (e.g., genomic and any omic template).

2. Methodology

In this section, we detail our GRN for boosting GNN based classifiers for neurological disorders diagnosis. Table 1 displays the mathematical notations that we use throughout this paper. We denote the matrices as boldface capital letters, e.g., $\mathbf{X}$, and scalars as lowercase letters, e.g., n. We illustrate in Fig. 2 the two proposed steps: (1) registration of input graphs into the population CBT and (2) classification of the registered brain graphs by the GRN plug-in.

Table 1
Major mathematical notations.

Mathematical notation	Definition
n_s	Total number of subjects
n	Total number of training subjects
n_r	Total number of regions of interest in the brain
n_{cbt}	Total number of independent brain graphs for CBT generation
$\mathbf{Y}^b$	Brain connectivity matrix of brain graph b
$\mathcal{O}$	Tensor $\in \mathbb{R}^{n_r \times n_r \times n_{cbt} \times n_{cbt}}$ comprising of high-order graphs $\mathcal{O}_{(i,j)}$, $1 \leq i, j \leq n_r$
$\mathcal{O}_{(i,j)}$	High-order graph $\in \mathbb{R}^{n_{cbt} \times n_{cbt}}$ defined for a ROI pair i and j
D	Tensor $\in \mathbb{R}^{n_r \times n_r \times n_{cbt}}$ comprising of distance vectors $D_{(i,j)}$
$D_{(i,j)}(b)$	Node weight of brain graph b in the high-order graph $\mathcal{O}_{(i,j)}$
$\mathbf{X}^{CBT}$	Connectional brain template connectivity matrix
$\mathbf{X}^{tr} = \{\mathbf{X}_1^{tr}, \ldots, \mathbf{X}_n^{tr}\}$	Training brain graph connectivity matrices $\in \mathbb{R}^{n \times n_r \times n_r}$
$\hat{\mathbf{X}}^{CBT} = \{\hat{\mathbf{X}}_1^{CBT}, \ldots, \hat{\mathbf{X}}_n^{CBT}\}$	Registered brain graph connectivity matrices $\in \mathbb{R}^{n \times n_r \times n_r}$
R	gGAN registration network
D	gGAN CBT-guided discriminator
$\mathcal{L}_{full}$	Full loss function
$\mathcal{L}_r$	Registration loss function
$\mathcal{L}_{adv}$	Adversarial loss function
$\mathcal{L}_{L_1}$	l_1 loss function
$\mathcal{L}_{gnn}$	Plug-in GNN loss function
λ	Coefficient of l_1 loss
V	A set of n_r nodes
E	A set of m_r directed or undirected edges
l	Index of layer
T^l	Transformation matrix $\in \mathbb{R}^{n_r \times d_l}$
L	Transformation matrix $\in \mathbb{R}^{m_r \times d_l}$
$\hat{\mathcal{N}}(i)$	The neighborhood containing all the adjacent vertices of vertex i
$T^l(i)$	Filtered signal of vertex $i \in \mathbb{R}^{d_l}$
F_{ji}^l	Filter generating network
ω^l	Weight parameter
b^l	Bias parameter

2.1. Connectional brain template (CBT) generation

A CBT is a brain graph template, which is normalized with respect to a population of brain graphs capturing the most centered, shared, and representative traits across a given brain graph population. It is also viewed as an average connectome and provides a representative map that holds the unique and distinctive connectivity patterns of a given population. Therefore, we assume that if a brain connectome can be registered to such a template with unique and distinctive features, the registered versions of the brain graphs can carry the individual connectivity patterns of each brain graph with respect to the population. There are several works in CBT derivation from a brain graph or multigraph populations (Rekik et al., 2017; Dhifallah and Rekik, 2019). A recent work (Gurbuz and Rekik, 2020) introduced Deep Graph Normalizer (DGN), the first GDL network to normalize a population of multi-view brain networks by integrating them into a single template. Dhifallah and Rekik (2020) proposed netNorm, which performs multi-view brain graph normalization to determine connectivities that are mostly affected by neurological disorders by comparing CBTs of different brain states (i.e., healthy *vs.* disordered). netNorm is designed for fusing a population of multi-view brain connectomes, where each brain is represented by a set of graphs, each capturing a particular connectional view of the brain. netNorm proposes a view-specific brain connectivity selection strategy where the most centered sample is selected for each pair of ROIs. This leads to the estimation of a centered population multiview graph. Next, a diffusion-based fusion strategy (Wang et al., 2014) is used to merge the view of the population graph, thereby producing the population CBT, encoded in a connectivity matrix. Without loss of generality, in this paper we use netNorm (Dhifallah and Rekik, 2020) to generate population CBTs. However, any other alternative approach can be adopted (Gurbuz and Rekik, 2020). Here, we learn the CBT using an *independent* brain graph dataset with n_{cbt} subjects.

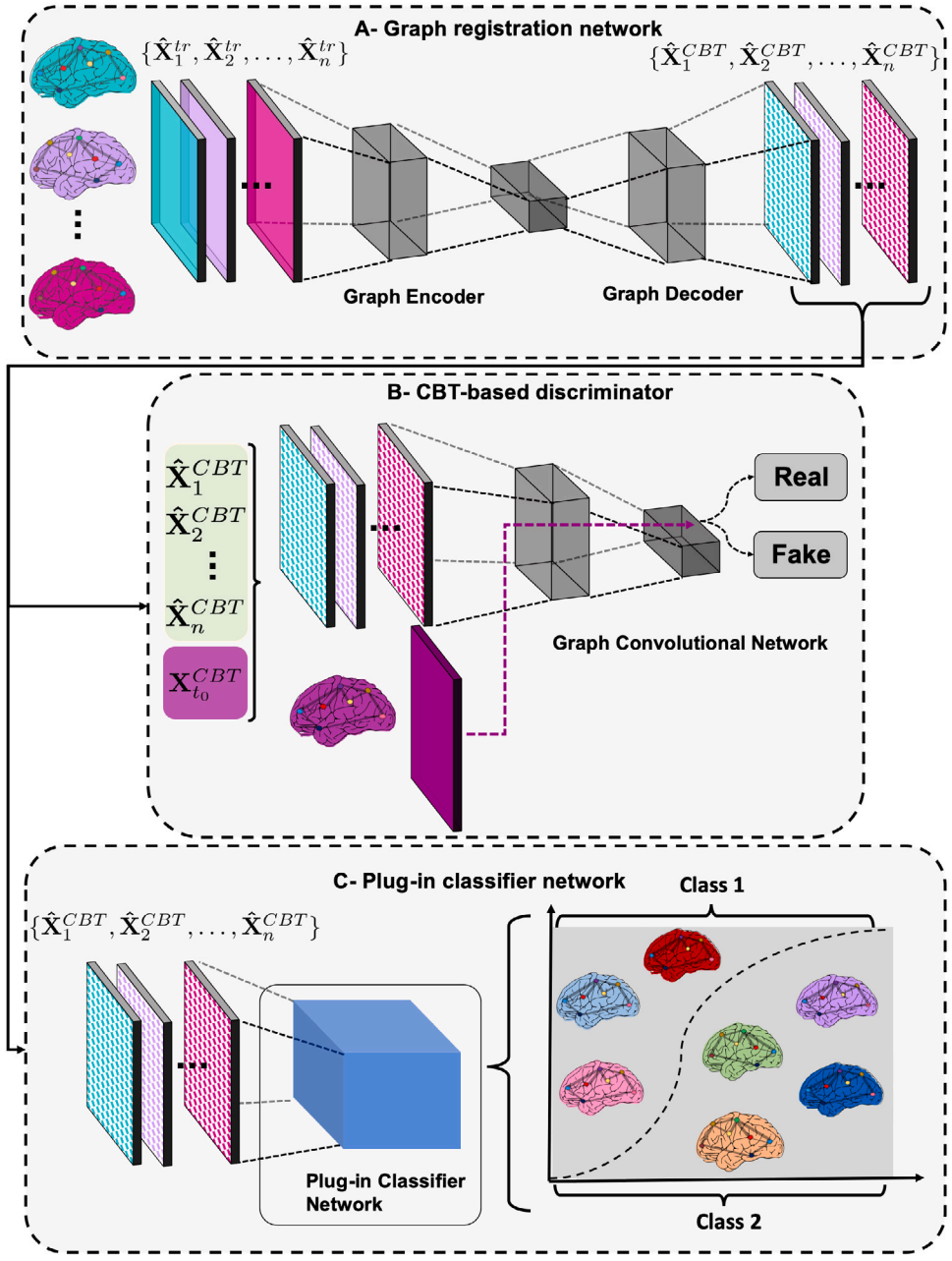

Fig. 2. *Proposed Template-based Graph Registration Network (GRN).* (A) *Graph registration network*. We propose a graph GAN (gGAN) architecture that learns to register brain graphs to a prior connectional brain template (CBT). We construct a three-layer graph convolutional neural network acting as an encoder–decoder that mimics a U-net architecture. Our registration network takes as input a set of n training brain graphs $\mathbf{X}^{tr}$ and outputs a set of $\hat{\mathbf{X}}^{CBT}$ sharing the same distribution as the prior CBT. (B) *CBT-based discriminator*. We design a two-layer graph convolutional neural network that differentiates between the real CBT and the registered brain graphs $\hat{\mathbf{X}}^{CBT}$. Basically, the discriminator decides whether the registered brain graph is a real CBT or not. **(C)** *GNN classifier*. We input the registered brain graphs $\hat{\mathbf{X}}^{CBT}$ to train a conventional graph neural network for classification.

We denote the connectivity between ROIs i and j $(1 \leq i, j \leq n_r)$ of a brain graph b as $\mathbf{Y}^b_{(i,j)}$ and define a tensor $\mathcal{O} \in \mathbb{R}^{n_r \times n_r \times n_{cbt} \times n_{cbt}}$ that consists of high-order graphs, $\mathcal{O}_{(i,j)} \in \mathbb{R}^{n_{cbt} \times n_{cbt}}$ (Dhifallah and Rekik, 2020). $\mathcal{O}_{(i,j)}$ holds the Euclidean distances across all brain graphs for each ROI pair i and j.

$$\mathcal{O}_{(i,j)}(b, b') = \sqrt{(\mathbf{Y}^b_{(i,j)} - \mathbf{Y}^{b'}_{(i,j)})^2}; \forall 1 \leq b, b' \leq n_{cbt} \tag{1}$$

For each brain graph b, we define a tensor $D \in \mathbb{R}^{n_r \times n_r \times n_{cbt}}$, where $D_{(i,j)}(b)$ holds the cumulative distance between brain graph b and other brain graphs in the population for each ROI pair connectivity (i, j), hence shows the topological weight of brain graph b in the high-order graph $\mathcal{O}_{(i,j)}$.

$$D_{(i,j)}(b) = \sum_{b'=1}^{n_{cbt}} \mathcal{O}_{(i,j)}(b, b') = \sum_{b'=1}^{n_{cbt}} \sqrt{(\mathbf{Y}^b_{(i,j)} - \mathbf{Y}^{b'}_{(i,j)})^2}; \forall 1 \leq b, b' \leq n_{cbt} \tag{2}$$

We assume that a pairwise connection of the closest brain graph to all other brain graphs in the population determines the most representative and centered connection. Therefore, for each brain connectivity (i, j), we select the connectivity weight of the brain graph with the minimum cumulative distance to all other brain graphs and construct the CBT as follows Dhifallah and Rekik (2020):

$$\mathbf{X}^{CBT}_{(i,j)} = \mathbf{Y}^k_{(i,j)}; \textit{where } k = \underset{1 \leq b \leq n_{cbt}}{\operatorname{argmin}} D_{(i,j)}(b) \tag{3}$$

2.2. Graph generative adversarial network (gGAN)

GANs are generative deep learning models that consist of two competing neural networks, namely a generator and a discriminator, first introduced by Goodfellow et al. (2014). The generator has an encoder–decoder architecture for learning how to generate fake output by mapping input data to a data distribution of interest while the discriminator learns to differentiate between ground-truth data and generated fake samples. While the discriminator learns to better discriminate between fake and real data, the generator tries to generate even more real-looking fake output to fool the discriminator. GANs are a good fit to registration task since they have excellent success in mimicking the original data distribution, thus they are the first choice when synthesizing any kind of data (Mahapatra, 2018; Zhang et al., 2020; Zheng et al., 2021). Further, the more successful the registration (mimicking the target data) is, the more individualized and well-represented graphs we obtain for the classification task. Therefore, we pursue with generative adversarial learning method in the registration process. A recent research (Gurler et al., 2020) proposed gGAN, the first graph-based GAN with a graph generator and a discriminator, which we leverage to design our registration network architecture. Our registration loss consists of an adversarial loss and an l_1 loss term. Since l_1 loss is effective in preserving general characteristics of the data and robust to sample outliers (Anagun et al., 2019), we further add the l_1 loss to improve the registered brain graph quality. Hence we express our registration loss function as follows:

$$\mathcal{L}_r = \mathcal{L}_{adv} + \lambda_l \mathcal{L}_{L1}(R) \tag{4}$$

This includes an adversarial loss optimized as follows Goodfellow et al. (2014):

$$\begin{aligned} \underset{R}{argmin}\underset{D}{max}\mathcal{L}_{adv} &= \mathbb{E}_{D(\mathbf{X}^{CBT})}[log\, D(\mathbf{X}^{CBT})] \\ &+\mathbb{E}_{D(\hat{\mathbf{X}}^{CBT})}[log(1 - D(R(\mathbf{X}^{CBT})))] \\ &+\mathbb{E}_{R(\mathbf{X}^{tr})}[log\, R(\mathbf{X}^{tr})] \end{aligned} \tag{5}$$

As shown in Fig. 2–A, our proposed GRN consists of a three-layer encoder–decoder graph convolutional neural network (GCN) inspired by the dynamic edge convolution operation introduced in Simonovsky and Komodakis (2017) and imitating a U-net architecture (Ronneberger et al., 2015) with skip connections, which enables feature reusability and enhances the decoding process by recovering some lost information with downsampling. GRN takes a set of $\mathbf{X}^{tr}$ training subjects as input and outputs a set of $\hat{\mathbf{X}}^{CBT}$, which share the same distribution as the fixed $\mathbf{X}^{CBT}$. Our graph registration network (Fig. 3) contains three graph convolutional neural network layers to which we apply batch normalization (Ioffe and Szegedy, 2015) and dropout (Xiao et al., 2016) to the output of each layer. These two operations make the network simplified and optimized helping to speed up network training and avoid overfitting.

We display the architecture of the discriminator in Figs. 2–B and 3. The discriminator is a two-layer graph neural network that takes as input the GRN output $\hat{\mathbf{X}}^{CBT}$ and outputs a tensor sized $\mathbb{R}^{n_r \times n_r}$. Also, to determine the realness of the registered graph, the discriminator takes the CBT itself $\mathbf{X}^{CBT}$ as input and outputs a tensor. Then these two tensors are sent to the adversarial loss function individually to obtain 2 values characterizing the *the realness* of $\hat{\mathbf{X}}^{CBT}$ and $\mathbf{X}^{CBT}$. The final discriminator loss is computed by averaging both losses.

In our GRN architecture, we use graph convolutional layers inspired by the dynamic graph-based edge convolution operation proposed by Simonovsky and Komodakis (2017). To perform this graph convolution operation, we represent a directed or undirected graph $G = (V, E)$ where V is a set of n_r ROIs and $E \subseteq V \times V$ is a set of m_r edges. Let l be the layer index in the neural network. We define two transformation matrices (i.e., functions) such as $\mathbf{T}^l : V \rightarrow \mathbb{R}^{d_l}$ and $\mathbf{L} : E \rightarrow \mathbb{R}^{d_s}$ where $\mathbf{T}^l \in \mathbb{R}^{n_r \times d_l}$ and $\mathbf{L} \in \mathbb{R}^{m_r \times d_s}$. d_s and d_l are dimensionality indexes. We define $\mathcal{N}(i) = \{j; (j,i) \in E\} \cup \{i\}$, which is considered as the neighborhood containing all the adjacent ROIs of a node i. The goal of each layer in both the registration network and the discriminator is to output the graph convolution result which can be considered as a filtered signal $\mathbf{T}^l(i) \in \mathbb{R}^{d_l}$ at node i. $\mathbf{T}^l$ is expressed as follows:

$$\mathbf{T}^l(i) = \frac{1}{\mathcal{N}(i)} \sum_{j \in \mathcal{N}(i)} \Theta^l_{ji} \mathbf{T}^{l-1}(j) + b^l, \tag{6}$$

where $\Theta^l_{ji} = F^l(L(j,i); \omega^l)$. $F^l : \mathbb{R}^{d_s} \rightarrow \mathbb{R}^{d_l \times d_{l-1}}$ is the filter generating network. We denote ω^l and b^l as model parameters that are updated only during training.

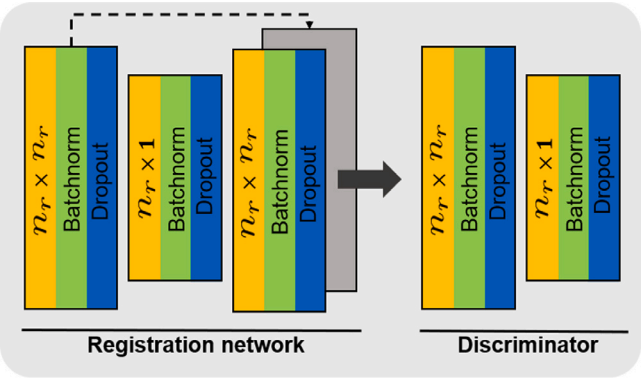

Fig. 3. *Illustration of the backbone network architecture of our graph registration network (GRN).* GRN consists of a registration network and a discriminator. The registration network is a three-layer graph convolutional neural network mimicking a U-net architecture with skip connections (Simonovsky and Komodakis, 2017; Ronneberger et al., 2015). The discriminator is a two-layer graph convolutional neural network. Each layer of the registration network and the discriminator consists of one dynamic edge convolution function followed by a BatchNorm, a ReLu, and a dropout operation except the discriminator's last activation function which is a sigmoid.

2.3. GNN classifier

To classify brain graphs in a population, we couple our plug-in GRN with a conventional GNN classification architecture (Fig. 1). In our paper, we use conventional GNNs such as GCN (Kipf and Welling, 2017), GAT (Veličković et al., 2018), DiffPool (Ying et al., 2019) and graph U-Nets (g-U-Nets) as classifier networks (Gao and Ji, 2019). We note that a few of these conventional GNNs, namely GCN and GAT, are not originally designed for graph-based classification task as they primarily classify nodes in graphs and not whole graphs (Bessadok et al., 2022). Therefore, in order to adapt both GNNs to be able to perform whole graph classification, we adapt them as follows. First, we design the output layer of the GCN as two nodes each one outputting the probability of the input graph belonging to the corresponding class. We add a linear layer to the GAT architecture that takes an input tensor of $\mathbb{R}^{n_r \times 1}$ to learn prediction logits for the whole graph. Before sending registered graphs to the target GNN, we apply mean-thresholding to the registered graphs. We compute the mean value of each graph and assign 0 to the values lower than the mean and 1 to the values greater than the mean. We assume that restricting values of the vertices to $\{0, 1\}$ provides simplicity in input data and helps GNN classifier better discriminate between classes and not overfit.

We input each registered brain graph $\hat{\mathbf{X}}^{CBT}$ to the target GNN to output a class label. Next, we compute the classification loss $\mathcal{L}_{gnn}$ of the GNN classifier. Our framework learns in an *end-to-end* fashion and uses a single loss function to optimize with a back-propagation process throughout the whole architecture. Therefore, we define the full loss function as a joint loss function composed of the registration loss $\mathcal{L}_r$ of the registration network and the GNN loss $\mathcal{L}_{gnn}$ of the GNN classifier as follows:

$$\mathcal{L}_{full} = \mathcal{L}_r + \lambda_c \mathcal{L}_{gnn} \tag{7}$$

GRN consists of dependent graph registration and graph classification steps. These fully dependent steps provide feedback to each other in order to globally optimize the graph classification process thanks to end-to-end training.

3. Results and discussion

Connectomic dataset. We evaluated our GRN plug-in on two datasets, where each subject is represented by a morphological brain graph. The first dataset (300) (ASD/NC dataset) is collected from the Autism Brain Imaging Data Exchange ABIDE I public dataset[2] and consists of 300 subjects: 150 normal controls (NC) and 150 subjects with autism spectrum disorder (ASD) (Martino et al., 2013; Soussia and Rekik, 2018). The second dataset (LMCI/AD dataset) is collected from Alzheimer's Disease Neuroimaging Initiative (ADNI) database GO public dataset[3] consisting of 77 subjects (Mahjoub et al., 2018): 36 subjects with Late Mild Cognitive Impairment (LMCI) and 41 subjects with Alzheimer disease (AD) (Mueller et al., 2005). The ADNI was launched in 2003 as a public–private partnership, led by Principal Investigator Michael W. Weiner, MD. The primary goal of ADNI has been to test whether serial magnetic resonance imaging (MRI), positron emission tomography (PET), other biological markers, and clinical and neuropsychological assessment can be combined to measure the progression of mild cognitive impairment (MCI) and early Alzheimer's disease (AD). We used FreeSurfer pipeline (Fischl, 2012) to reconstruct both right and left cortical hemispheres (RH and LH) for each subject from structural T1-weighted MRI. We parcellated each hemisphere into 35 cortical regions of interest using Desikan-Killiany atlas (Fischl, 2004). Next, for each cortical ROI, we compute the average cortical thickness across its vertices. A morphological connectivity weight between two ROIs is then computed as the absolute difference between their corresponding average cortical thickness values. Morphological brain networks have gained momentum over the last few years where brain connectivity is generated from conventional T1-weighted MRI and morphological dissimilarities are quantified between brain regions (Soussia and Rekik, 2018; Mahjoub et al., 2018; Nebli and Rekik, 2019; Bilgen et al., 2020; Yalçin and Rekik, 2021)

Parameter setting. We empirically tuned and set λ_l for the registration network to 250 to balance the range difference between the two losses and also increase the impact of the L1 loss compared to the adversarial loss. Further, we varied and empirically set λ_c of the GNN to inhibit the GRN from dominating the back-propagation and introducing drastic changes in the brain graph registration operation. Hence, the plug-in GNN learning remains steady when trained on the registered brain graphs, which slightly changes in each run as a result of end-to-end learning. We note that this parameter can be tuned differently based on the input graph dataset. We chose ADAM (Kingma and Ba, 2014) as our default optimizer and set the learning rate at 0.0001 for the GNN and 0.0001 for the registration network, 0.001 for the discriminator of the gGAN. We set the exponential decay rate for the first-moment estimates (i.e., beta 1) to 0.5, and the exponential decay rate for the second-moment estimates (i.e., beta 2) to 0.999 for the ADAM optimizer. We set the weight decay of GCN and GAT to 0.00005 and 0.00001 for DiffPool and g-U-Nets. We use the same learning rates and weight decay values for the benchmarking conventional GNN classifiers. Lastly, other parameters, for instance, the number of epochs or the number of neurons of the hidden layers for the corresponding GNNs are varied by applying hyper-parameter tuning for each dataset.

Comparison methods. We compared our framework with the conventional GNNs respectively GCN, GAT, DiffPool, and g-U-Nets that are used as classifiers in our framework to evaluate the impact on classification accuracy.

Evaluation. We evaluate our framework using 5-fold cross-validation (CV) and report the mean prediction results. We also use 5-fold CV to evaluate the benchmark methods (Kipf and Welling, 2017; Veličković et al., 2018; Ying et al., 2019; Gao and Ji, 2019).

Results and benchmarking. In this work, we proposed GRN, a geometric deep learning framework that has a graph registration network plugged into a target graph neural network. First, our registration network registers brain graphs to a prior connectional brain template (CBT) where the distribution of each input brain graph is aligned with that of the given CBT. Second, the GNN of our framework is trained using the registered brain graphs to predict their class labels. These two networks work together dependently by back-propagating with a joint loss and learn from each other in this wise.

We firstly report the Principal Component Analysis (PCA) projection of the brain graphs and their registered versions for ASD/NC connectional dataset in Fig. 4 to evaluate between-class separability of registered brain graphs. We also display the CBT projection in yellow with the original brain graphs and also their registered versions. We show that the registered brain graphs of both classes are more separable than the original brain graphs.

We conducted sixteen different experiments, using two datasets with left and right hemisphere and four conventional GNNs as classification networks. For each dataset, we trained them with four different GNN classifiers to our registration network. Then, we trained each dataset with the four classifiers without using the registration network to evaluate the impact on the brain graph classification accuracy. As shown in Table 2, our GRN model remarkably boosted the prediction accuracy of conventional GNN methods resulting in 75% accuracy increase in 12 out of 16 experiments. Furthermore, our method was successful in both ASD/NC and AD/LMCI datasets, which implies that GRN can handle heterogeneous data distributions. Hence, it is generalizable to any task. Also, results show that our graph registration network model outperformed four different kinds of GNNs, which indicates that GRN can work with any GNN that aims to handle any other task such as link prediction, graph regression, and node classification to boost its performance. Overall, our graph registration strategy achieved remarkable performance in brain graph classification task and showed that graph registration to a prior graph template (i.e., CBT) is highly recommended for graph-based learning tasks.

Biological markers of ASD/NC population. We further investigated our experiment results to identify connectional biomarkers that distinguish between Autism (ASD) and normal control (NC) brains. As we aim to find the most discriminative biomarkers, we select the method with the highest prediction performance for each dataset. Next, we extract their learned weights to display the discriminative power of each brain ROI between ASD and NC as displayed in Fig. 5. For the left hemisphere, According to Table 2, we chose GRN with GCN, which resulted in 57.08% prediction accuracy as the best among all methods. We discovered that the isthmus-cingulate cortex and insula cortex are the most discriminative biomarkers for autism. The isthmus-cingulate cortex is responsible for social behavior impairment and abnormal functional activity in social tasks in ASD (Doyle-Thomas et al., 2012). Also, hypoactivation and dysconnectivity during emotional and social tasks in ASD are associated with dysfunctional insula cortex by many researches (Di Martino et al., 2009; Bird et al., 2010). For the right hemisphere (RH), we drive the learned weights of GCN since GCN had the best prediction accuracy of 57.7%. We selected the ROIs with the most discriminative power such as lateral orbital frontal cortex and posterior cingulate cortex. We indicate that the human brain has hemispheric asymmetries that naturally develop (Wada et al.,

[2] $http://fcon_1000.projects.nitrc.org/indi/abide/.

[3] Data used in preparation of this article were obtained from the Alzheimer's Disease Neuroimaging Initiative (ADNI) database (adni.loni.usc.edu). As such, the investigators within the ADNI contributed to the design and implementation of ADNI and/or provided data but did not participate in analysis or writing of this report. A complete listing of ADNI investigators can be found at: https://adni.loni.usc.edu/wp-content/uploads/how_to_apply/ADNI_Acknowledgement_List.pdf.

Table 2
Prediction accuracy (Acc), precision (Prec), and recall (Rec) of GRN combined with benchmark GNNs and benchmark GNNs themselves. We emphasize in bold the best performing method for each GNN architecture. ASD: autism spectrum disorder. NC: normal control. AD: Alzheimer's disease. LMCI: late mild cognitive impairment. LH: Left hemisphere. RH: Right hemisphere. WB: whole brain.

Datasets	ASD/NC									AD/LMCI								
	LH			RH			WB			LH			RH			WB		
	Acc	Prec	Rec	Acc	Prec	Rec	Acc	Prec	Rec	Acc	Prec	Rec	Acc	Prec	Rec	Acc	Prec	Rec
GRN(GCN)	**57.08**	**56.75**	**56.6**	57	56.67	56.66	**57.4**	**57.1**	**57.083**	**54.15**	**54.31**	**54.28**	**53.86**	**54.31**	**54.28**	**54.005**	**53.78**	**53.80**
GCN (Kipf and Welling, 2017)	52.5	52.52	52.5	**57.7**	**57.51**	**57.5**	55.1	55.15	55	52.46	52.08	52.083	50.46	50.42	50.41	51.46	51.25	51.24
GRN(GAT)	49.67	49.58	49.58	56.25	56.28	56.25	52.96	52.95	52.91	**55.08**	**54.62**	**54.52**	**53.54**	**52.36**	**52.38**	**54.31**	**53.78**	**53.80**
GAT (Veličković et al., 2018)	**56.66**	56.28	56.25	**57.5**	57.52	57.5	**57.08**	**56.68**	**56.66**	**53.84**	51.91	51.90	48.52	47.1	47.14	51.18	51.75	51.66
GRN(DiffPool)	**53.75**	**53.79**	**53.75**	**56.3**	**56.28**	**56.25**	**55.025**	**55.05**	**55**	55.54	54.75	54.52	**52.42**	**52.89**	**52.85**	**53.98**	**53.2**	**53.09**
DiffPool (Ying et al., 2019)	53.3	52.93	52.91	53.47	53.34	53.33	53.33	52.92	52.91	**59.84**	**58.3**	**58.33**	47.53	46.42	46.42	53.685	52.36	52.38
GRN(g-U-Nets)	**52.94**	**52.916**	**52.462**	**51.99**	**51.68**	**51.66**	**52.465**	**52.09**	**52.08**	**64.46**	**63.02**	**63.09**	**52.81**	**52.36**	**52.38**	**58.635**	**58.3**	**58.33**
g-U-Nets (Gao and Ji, 2019)	49.59	49.58	49.58	51.17	50.85	50.83	50.38	50	50	57.23	60.85	65	37.23	44.3	42.66	47.23	40.38	37

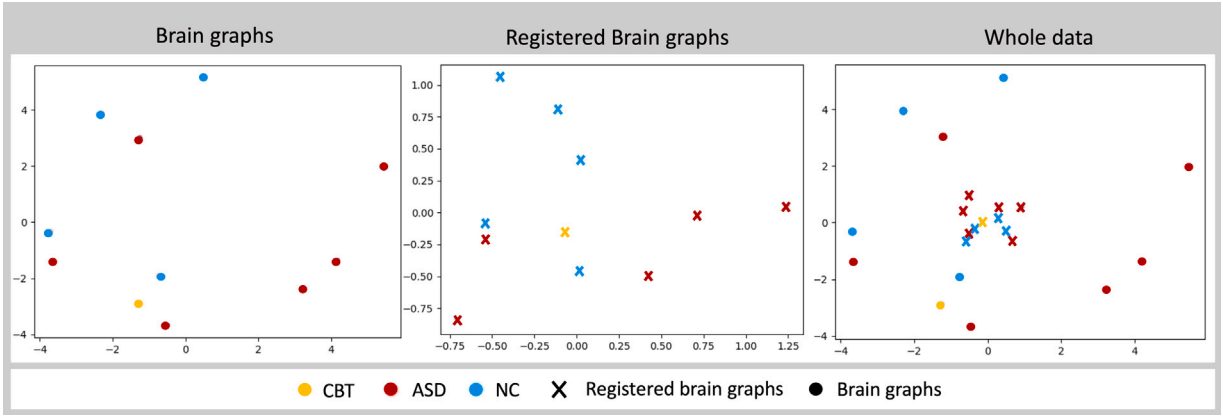

Fig. 4. The Principal Component Analysis (PCA) projection of the brain graphs and their registered versions along with the CBT.

1975) or through the asymmetric alteration under the influence of autism (Chiron et al., 1995; Herbert et al., 2005), which explains the different biomarker findings for the left and right hemisphere. According to Watanabe et al. (2014), restricted and repetitive behaviors in ASD is linked with lateral orbital frontal cortex. Additionally, Hau et al. (2019) states that there is a significant alteration in development trajectory in ASD compared to NC in the right hemisphere while both groups followed a similar development in the left hemisphere.

Biological markers of AD/LMCI population. As shown in Table 2, GRN with g-U-Nets was the most successful method out of all methods as it achieved 64.46% classification accuracy for the left hemisphere (LH) of AD/LMCI dataset. Note that this is a very difficult classification task since the brain undergoes *subtle* changes between both LMCI and AD states—these are difficult to tease apart (Dhifallah and Rekik, 2020). The two most discriminative biomarkers were the unmeasured corpus callosum and superior frontal gyrus (Fig. 5). Changes in the corpus callosum that are already present in LMCI continue to expand in AD (Di Paola et al., 2010), which justifies the discriminative power of the corpus callosum. Likewise, the superior frontal gyrus, which is known to be laboriously responsible for various cognitive and motor control tasks (Boisgueheneuc et al., 2006; Li et al., 2013), marked the difference between LMCI and AD patients and is considered as one of the strong biomarkers of LMCI patient conversion to Alzheimer's disease (AD) (Drzezga et al., 2003). As for the right hemisphere (RH), we select (GRN + GCN) architecture which achieved a 53.86% classification accuracy and we identify the isthmus-cingulate cortex and bank of the superior temporal sulcus as the most discriminative ROIs. The isthmus-cingulate cortex is associated with cognitive decline and executive dysfunction (Wei et al., 2018) and hemispheric asymmetry was better preserved in the bank of the superior temporal sulcus in MCI but lost in AD patients (Long et al., 2013).

Limitations and recommendations for future work. Although our graph registration network produced the best results in a variety of brain graph classification tasks, there are a few limitations that we are keen to point out for further investigation. First, the proposed GRN particularly works on uni-modal brain graphs with only one edge type, which overlooks the multigraph representation of brain connectivity that better models different types of interactions between brain regions (Gürbüz and Rekik, 2021; Chaari et al., 2020; Banka et al., 2020). Specifically, edge types can vary according to deployed connectivity measures for modeling the relation between brain regions such as morphological dissimilarity derived from structural T1-weighted MRI or functional connectivity derived from resting-state functional MRI—to name just a few. Therefore, we aim to optimize our GRN model to operate on multi-modal brain graphs in order to capture the relational connectomic features. Second, we use netNorm (Dhifallah and Rekik, 2019) to construct a connectional brain template (CBT) for the target registration task. netNorm uses a simple multigraph population processing pipeline that is dichotomized into different stages, each optimized individually. This might lead to error accumulation throughout the whole pipeline. To address this weakness, recently (Gurbuz and Rekik, 2020) proposed the deep graph normalizer (DGN), which is the first GNN architecture for normalizing a population of brain graphs to integrate them into a CBT. Since our framework is generic, the user has the liberty to test more advanced CBT estimation methods such as Gurbuz and Rekik (2020), Gürbüz and Rekik (2021).

4. Conclusion

In this paper, we proposed a template-based graph registration network that can be used as a plug-in to boost the performance of graph neural network architectures. Our model is composed of two major parts, respectively a graph registration network (GRN) and a

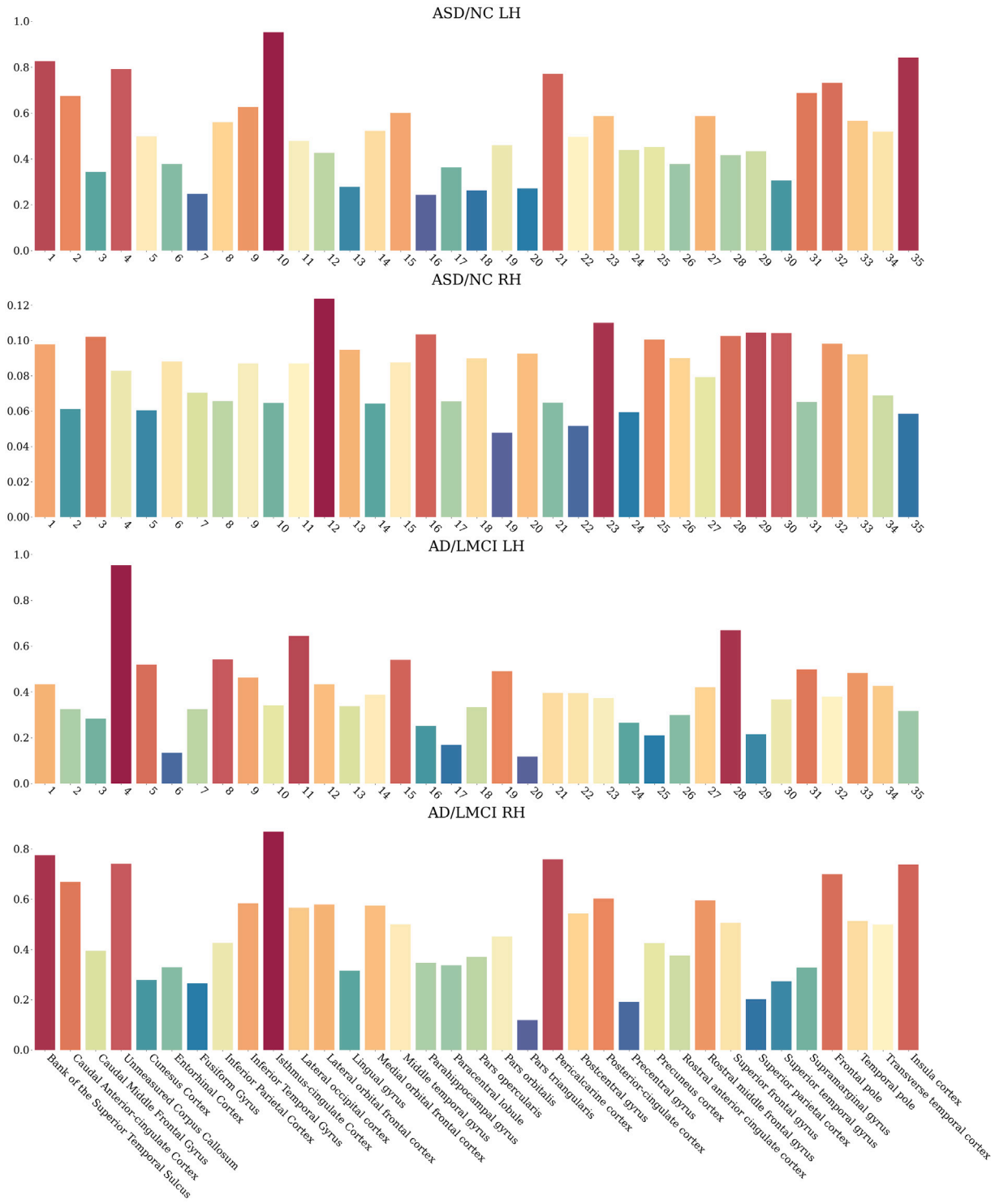

Fig. 5. *The learned weights for each cortical region by the best performing method for the four datasets.* ASD: autism spectrum disorder. NC: normal control. AD: Alzheimer's disease. LMIC: late mild cognitive impairment. LH: left hemisphere. RH: right hemisphere.

GNN. GRN is a gGAN, which registers each input brain graph to a prior connectional brain template (CBT) to enhance their individual connectivity features. Both networks are trained in an end-to-end fashion while optimizing a joint loss function. Our results showed that GRN remarkably boosts the classification accuracy of GNN models across 4 clinical datasets and hence is a successful framework for brain graph classification. Our plug-in GRN is a generic model. It can be trained using any type of graph templates (e.g., genomic and any omic template) and can be coupled with any GNN architecture. In our future work, we will extend our GRN to handle multi-modal brain graphs for a better modeling of the multiple interaction types between brain regions.

Code availability

An open-source Python implementation of GRN is available on GitHub at https://github.com/basiralab/GRN. The release includes a demo using simulated data and notes regarding Python packages, which need to be installed. Information regarding input format can be also found in the same repository.

CRediT authorship contribution statement

Zeynep Gürler: Methodology, Formal analysis, Validation, Visualization, Writing – original draft, Writing – review & editing. **Mohammed Amine Gharsallaoui:** Formal analysis, Writing – original draft. **Islem Rekik:** Conceptualization, Supervision, Methodology, Resources, Writing – review & editing, Funding acquisition.

Declaration of competing interest

The authors declare that they have no known competing financial interests or personal relationships that could have appeared to influence the work reported in this paper.

Data availability

The data that support the findings of this study are publicly available from ADNI data (http://adni.loni.usc.edu/). For reproducibility and comparability, the authors will make available upon request all morphological networks generated based on the four cortical attributes (maximum principal curvature, cortical thickness, sulcal depth, and average curvature) for the 77 subjects (41 AD and 36 LMCI) following the approval by ADNI Consortium. Our large-scale dataset is also available from the public ABIDE initiative (http://fcon_1000.projects.nitrc.org/indi/abide/). Following the approval by the ABIDE initiative, all morphological networks generated from the six cortical attributes (cortical surface area and minimum principle area in addition to 4 aforementioned measures) for the 300 subjects (150 NC and 150 ASD) are also accessible from the authors upon request.

Acknowledgments

This work was funded by generous grants from the European H2020 Marie Sklodowska-Curie action (grant no. 101003403, http://basira-lab.com/normnets/) to I.R. and the Scientific and Technological Research Council of Turkey to I.R. under the TUBITAK 2232 Fellowship for Outstanding Researchers (no. 118C288, http://basira-lab.com/reprime/). However, all scientific contributions made in this project are owned and approved solely by the authors. M.A.G is supported by the same TUBITAK 2232 Fellowship.

Data collection and sharing for this project was funded by the Alzheimer's Disease Neuroimaging Initiative (ADNI) (National Institutes of Health Grant U01 AG024904) and DOD ADNI (Department of Defense award number W81XWH-12-2-0012). ADNI is funded by the National Institute on Aging, the National Institute of Biomedical Imaging and Bioengineering, and through generous contributions from the following: AbbVie, Alzheimer's Association; Alzheimer's Drug Discovery Foundation; Araclon Biotech; BioClinica, Inc.; Biogen; Bristol-Myers Squibb Company; CereSpir, Inc.; Cogstate; Eisai Inc.; Elan Pharmaceuticals, Inc.; Eli Lilly and Company; EuroImmun; F. Hoffmann-La Roche Ltd and its affiliated company Genentech, Inc.; Fujirebio; GE Healthcare; IXICO Ltd.; Janssen Alzheimer Immunotherapy Research & Development, LLC.; Johnson & Johnson Pharmaceutical Research & Development LLC.; Lumosity; Lundbeck; Merck & Co., Inc.; Meso Scale Diagnostics, LLC.; NeuroRx Research; Neurotrack Technologies; Novartis Pharmaceuticals Corporation; Pfizer Inc.; Piramal Imaging; Servier; Takeda Pharmaceutical Company; and Transition Therapeutics. The Canadian Institutes of Health Research is providing funds to support ADNI clinical sites in Canada. Private sector contributions are facilitated by the Foundation for the National Institutes of Health (www.fnih.org). The grantee organization is the Northern California Institute for Research and Education, and the study is coordinated by the Alzheimer's Therapeutic Research Institute at the University of Southern California. ADNI data are disseminated by the Laboratory for Neuro-Imaging at the University of Southern California.

References

Anagun, Y., Isik, S., Seke, E., 2019. SRLibrary: Comparing different loss functions for super-resolution over various convolutional architectures. J. Vis. Commun. Image Represent. 61, 178–187.

Asiri, N., Hussain, M., Al Adel, F., Alzaidi, N., 2019. Deep learning based computer-aided diagnosis systems for diabetic retinopathy: A survey. Artif. Intell. Med. 99, 101701.

Balakrishnan, G., Zhao, A., Sabuncu, M.R., Guttag, J., Dalca, A.V., 2019. VoxelMorph: A learning framework for deformable medical image registration. IEEE Trans. Med. Imaging 38 (8), 1788–1800.

Banka, A., Buzi, I., Rekik, I., 2020. Multi-view brain HyperConnectome AutoEncoder for brain state classification. In: International Workshop on Predictive Intelligence in Medicine. Springer, pp. 101–110.

Bessadok, A., Mahjoub, M.A., Rekik, I., 2022. Graph neural networks in network neuroscience. IEEE Trans. Pattern Anal. Mach. Intell..

Bilgen, I., Guvercin, G., Rekik, I., 2020. Machine learning methods for brain network classification: Application to autism diagnosis using cortical morphological networks. J. Neurosci. Methods 343, 108799.

Bird, G., Silani, G., Brindley, R., White, S., Frith, U., Singer, T., 2010. Empathic brain responses in insula are modulated by levels of alexithymia but not autism. Brain 133 (5), 1515–1525.

Boisgueheneuc, F.d., Levy, R., Volle, E., Seassau, M., Duffau, H., Kinkingnehun, S., Samson, Y., Zhang, S., Dubois, B., 2006. Functions of the left superior frontal gyrus in humans: a lesion study. Brain 129 (12), 3315–3328.

Bove, P., Micheli, A., Milazzo, P., Podda, M., 2020. Prediction of dynamical properties of biochemical pathways with graph neural networks. Bioinformatics 32–43.

Chaari, N., Akdağ, H.C., Rekik, I., 2020. Estimation of gender-specific connectional brain templates using joint multi-view cortical morphological network integration. Brain Imaging Behav. 1–20.

Chiron, C., Leboyer, M., Leon, F., Jambaqué, I., Nuttin, C., Syrota, A., 1995. SPECT of the brain in childhood autism: evidence for a lack of normal hemispheric asymmetry. Dev. Med. Child Neurol..

Davatzikos, C., Zacharaki, E.I., Gooya, A., Clark, V., 2011. Multi-parametric analysis and registration of brain tumors: constructing statistical atlases and diagnostic tools of predictive value. In: 2011 Annual International Conference of the IEEE Engineering in Medicine and Biology Society. IEEE, pp. 6979–6981.

de Vos, B.D., Berendsen, F.F., Viergever, M.A., Sokooti, H., Staring, M., Išgum, I., 2019. A deep learning framework for unsupervised affine and deformable image registration. Med. Image Anal. 52, 128–143.

Dhifallah, S., Rekik, I., 2019. Clustering-based multi-view network fusion for estimating brain network atlases of healthy and disordered populations. J. Neurosci. Methods 311, 426–435.

Dhifallah, S., Rekik, I., 2020. Estimation of connectional brain templates using selective multi-view network normalization. Med. Image Anal. 59, 101567.

Di Martino, A., Ross, K., Uddin, L., Sklar, A., Castellanos, F., Milham, M., 2009. Functional brain correlates of social and nonsocial processes in autism spectrum disorders: an activation likelihood estimation meta-analysis. Biol. Psychiatry.

Di Paola, M., Di Iulio, F., Cherubini, A., Blundo, C., Casini, A., Sancesario, G., Passafiume, D., Caltagirone, C., Spalletta, G., 2010. When, where, and how the corpus callosum changes in MCI and AD. Neurology 74 (14), 1136–1142, https://n.neurology.org/content/74/14/1136.

Diehl, F., Brunner, T., Le, M.T., Knoll, A., 2019. Graph neural networks for modelling traffic participant interaction. In: 2019 IEEE Intelligent Vehicles Symposium (IV). pp. 695–701.

Doyle-Thomas, K.A., Kushki, A., Duerden, E.G., Taylor, M.J., Lerch, J.P., Soorya, L.V., Wang, A.T., Fan, J., Anagnostou, E., 2012. The effect of diagnosis, age, and symptom severity on Cortical Surface Area in the cingulate cortex and insula in autism spectrum disorders. J. Child Neurol. 28 (6), 732–739.

Drzezga, A., Lautenschlager, N., Siebner, H., Riemenschneider, M., Willoch, F., Minoshima, S., Schwaiger, M., Kurz, A., 2003. Cerebral metabolic changes accompanying conversion of mild cognitive impairment into Alzheimer's disease: a PET follow-up study. Eur. J. Nucl. Med. Mol. Imaging 30, 1104–1113.

Du, Y., Fu, Z., Calhoun, V.D., 2018. Classification and prediction of brain disorders using functional connectivity: Promising but challenging. Front. Neurosci. 12, 525.

Fan, Y., Rao, H., Giannetta, J., Hurt, H., Wang, J., Davatzikos, C., Shen, D., 2006. Diagnosis of brain abnormality using both structural and functional MR images. In: 2006 International Conference of the IEEE Engineering in Medicine and Biology Society. IEEE, pp. 1044–1047.

Fischl, B., 2004. Automatically parcellating the human cerebral cortex. Cerebral Cortex 14 (1), 11–22.

Fischl, B., 2012. FreeSurfer. NeuroImage 62 (2), 774–781, 20 YEARS OF fMRI.
Fornito, A., Zalesky, A., Breakspear, M., 2015. The connectomics of brain disorders. Nat. Rev. Neurosci. 16 (3), 159–172.
Gafuroglu, C., Rekik, I., 2019. Image evolution trajectory prediction and classification from baseline using learning-based patch atlas selection for early diagnosis. arXiv preprint arXiv:1907.06064.
Gao, H., Ji, S., 2019. Graph u-nets. In: International Conference on Machine Learning. PMLR, pp. 2083–2092.
Goodfellow, I., Pouget-Abadie, J., Mirza, M., Xu, B., Warde-Farley, D., Ozair, S., Courville, A., Bengio, Y., 2014. Generative adversarial nets. Adv. Neural Inf. Process. Syst. 2672–2680.
Gurbuz, M.B., Rekik, I., 2020. Deep graph normalizer: A geometric deep learning approach for estimating connectional brain templates. In: Martel, A.L., Abolmaesumi, P., Stoyanov, D., Mateus, D., Zuluaga, M.A., Zhou, S.K., Racoceanu, D., Joskowicz, L. (Eds.), Medical Image Computing and Computer Assisted Intervention – MICCAI 2020. Springer International Publishing, Cham, pp. 155–165.
Gürbüz, M.B., Rekik, I., 2021. MGN-net: A multi-view graph normalizer for integrating heterogeneous biological network populations. Med. Image Anal. 71, 102059.
Gurler, Z., Nebli, A., Rekik, I., 2020. Foreseeing brain graph evolution over time using deep adversarial network normalizer. arXiv:2009.11166.
Hamilton, W.L., Ying, R., Leskovec, J., 2018. Inductive representation learning on large graphs. arXiv:1706.02216.
Hau, J., Aljawad, S., Baggett, N., Fishman, I., Carper, R.A., Müller, R.A., 2019. The cingulum and cingulate U-fibers in children and adolescents with autism spectrum disorders. Hum. Brain Mapp..
Herbert, M.R., Ziegler, D.A., Deutsch, C., O'Brien, L.M., Kennedy, D.N., Filipek, P., Bakardjiev, A., Hodgson, J., Takeoka, M., Makris, N., et al., 2005. Brain asymmetries in autism and developmental language disorder: a nested whole-brain analysis. Brain 128 (1), 213–226.
Hu, Y., Modat, M., Gibson, E., Li, W., Ghavami, N., Bonmati, E., Wang, G., Bandula, S., Moore, C.M., Emberton, M., Ourselin, S., Noble, J.A., Barratt, D.C., Vercauteren, T., 2018. Weakly-supervised convolutional neural networks for multimodal image registration. Med. Image Anal. 49, 1–13.
Ioffe, S., Szegedy, C., 2015. Batch normalization: Accelerating deep network training by reducing internal covariate shift. arXiv preprint arXiv:1502.03167.
Khazaee, A., Ebrahimzadeh, A., Babajani-Feremi, A., 2015. Application of advanced machine learning methods on resting-state fMRI network for identification of mild cognitive impairment and Alzheimer's disease.
Kim, M., Wu, G., Rekik, I., Shen, D., 2016. Dual-layer groupwise registration for consistent labeling of longitudinal brain images. In: International Workshop on Machine Learning in Medical Imaging. Springer, pp. 69–76.
Kingma, D.P., Ba, J., 2014. Adam: A method for stochastic optimization. arXiv:1412.6980.
Kipf, T.N., Welling, M., 2017. Semi-supervised classification with graph convolutional networks. arXiv:1609.02907.
Lee, J.-G., Jun, S., Cho, Y.-W., Lee, H., Kim, G.B., Seo, J.B., Kim, N., 2017. Deep learning in medical imaging: general overview. Korean J. Radiol. 18 (4), 570.
Li, W., Qin, W., Liu, H., Fan, L., Wang, J., Jiang, T., Yu, C., 2013. Subregions of the human superior frontal gyrus and their connections. NeuroImage.
Li, Z., Shen, X., Jiao, Y., Pan, X., Zou, P., Meng, X., Yao, C., Bu, J., 2020. Hierarchical bipartite graph neural networks: Towards large-scale E-commerce applications. In: 2020 IEEE 36th International Conference on Data Engineering (ICDE). pp. 1677–1688.
Li, G., Wang, L., Yap, P.-T., Wang, F., Wu, Z., Meng, Y., Dong, P., Kim, J., Shi, F., Rekik, I., et al., 2019. Computational neuroanatomy of baby brains: A review. NeuroImage 185, 906–925.
Liu, M., Zhang, D., Shen, D., Alzheimer's Disease Neuroimaging Initiative, 2015. View-centralized multi-atlas classification for Alzheimer's disease diagnosis. Hum. Brain Mapp. 36 (5), 1847–1865.
Long, X., Zhang, L., Liao, W., Jiang, C., Qiu, B., 2013. Alzheimer's disease neuroimaging initiative. Distinct laterality alterations distinguish mild cognitive impairment and Alzheimer's disease from healthy aging: statistical parametric mapping with high resolution MRI. Hum Brain Mapp..
Mahapatra, D., 2018. GAN based medical image registration. arXiv preprint arXiv:1805.02369.
Mahjoub, I., Mahjoub, M.A., Rekik, I., 2018. Brain multiplexes reveal morphological connectional biomarkers fingerprinting late brain dementia states. Sci. Rep. 8 (1), 4103.
Mallick, T., Balaprakash, P., Rask, E., Macfarlane, J., 2020. Transfer learning with graph neural networks for short-term highway traffic forecasting. arXiv:2004.08038.
Martino, A.D., Yan, C.-G., Li, Q., Denio, E., Castellanos, F.X., Alaerts, K., Anderson, J.S., Assaf, M., Bookheimer, S.Y., Dapretto, M., et al., 2013. The autism brain imaging data exchange: towards a large-scale evaluation of the intrinsic brain architecture in autism. Mol. Psychiatry 19 (6), 659–667.
Min, R., Wu, G., Cheng, J., Wang, Q., Shen, D., Alzheimer's Disease Neuroimaging Initiative, 2014. Multi-atlas based representations for Alzheimer's disease diagnosis. Hum. Brain Mapp. 35 (10), 5052–5070.
Mueller, S.G., Weiner, M.W., Thal, L.J., Petersen, R.C., Jack, C., Jagust, W., Trojanowski, J.Q., Toga, A.W., Beckett, L., 2005. The Alzheimer's disease neuroimaging initiative. NeuroImaging Clin. North Am. 15 (4), 869–877, Alzheimer's Disease: 100 Years of Progress.
Nebli, A., Rekik, I., 2019. Gender differences in cortical morphological networks. Brain Imaging Behav. 1–9.
Rekik, I., Li, G., Lin, W., Shen, D., 2017. Estimation of brain network atlases using diffusive-shrinking graphs: Application to developing brains. In: Niethammer, M., Styner, M., Aylward, S., Zhu, H., Oguz, I., Yap, P.-T., Shen, D. (Eds.), Information Processing in Medical Imaging. Springer International Publishing, Cham, pp. 385–397.
Richiardi, J., Achard, S., Bunke, H., Van De Ville, D., 2013. Machine learning with brain graphs: Predictive modeling approaches for functional imaging in systems neuroscience. IEEE Signal Process. Mag. 30 (3), 58–70.
Ronneberger, O., Fischer, P., Brox, T., 2015. U-net: Convolutional networks for biomedical image segmentation. CoRR abs/1505.04597. arXiv:1505.04597.
Simonovsky, M., Komodakis, N., 2017. Dynamic edge-conditioned filters in convolutional neural networks on graphs. CoRR abs/1704.02901. arXiv:1704.02901.
Sokooti, H., de Vos, B., Berendsen, F., Lelieveldt, B.P.F., Išgum, I., Staring, M., 2017. Nonrigid image registration using multi-scale 3D convolutional neural networks. In: Descoteaux, M., Maier-Hein, L., Franz, A., Jannin, P., Collins, D.L., Duchesne, S. (Eds.), Medical Image Computing and Computer Assisted Intervention MICCAI 2017. Springer International Publishing, Cham, pp. 232–239.
Soussia, M., Rekik, I., 2018. Unsupervised manifold learning using high-order morphological brain networks derived from T1-w MRI for Autism Diagnosis. Front. Neuroinform. 12.
Suzuki, K., 2017. Overview of deep learning in medical imaging. Radiol. Phys. Technol. 10 (3), 257–273.
van den Heuvel, M.P., Sporns, O., 2019. A cross-disorder connectome landscape of brain dysconnectivity. Nat. Rev. Neurosci. 20 (7), 435–446.
Veličković, P., Cucurull, G., Casanova, A., Romero, A., Liò, P., Bengio, Y., 2018. Graph attention networks. arXiv:1710.10903.
Wada, J.A., Clarke, R., Hamm, A., 1975. Cerebral hemispheric asymmetry in humans: Cortical speech zones in 100 adult and 100 infant brains. Arch Neurol..
Wang, B., Mezlini, A.M., Demir, F., Fiume, M., Tu, Z., Brudno, M., Haibe-Kains, B., Goldenberg, A., 2014. Similarity network fusion for aggregating data types on a genomic scale. Nature Methods 11 (3), 333.
Watanabe, H., Nakamura, M., Ohno, T., Itahashi, T., Tanaka, E., Ohta, H., Yamada, T., Kanai, C., Iwanami, A., Kato, N., et al., 2014. Altered orbitofrontal sulcogyral patterns in adult males with high-functioning autism spectrum disorders. Soc. Cognit. Affect. Neurosci. 9 (4), 520–528.
Wei, H., Kong, M., Zhang, C., Guan, L., Ba, M., Alzheimer's Disease Neuroimaging Initiative, 2018. The structural MRI markers and cognitive decline in prodromal Alzheimer's disease: a 2-year longitudinal study. Quant. Imaging Med. Surg. 8 (10).
Xiao, T., Li, H., Ouyang, W., Wang, X., 2016. Learning deep feature representations with domain guided dropout for person re-identification. In: Proceedings of the IEEE Conference on Computer Vision and Pattern Recognition. pp. 1249–1258.
Yalçin, A., Rekik, I., 2021. A diagnostic unified classification model for classifying multi-sized and multi-modal brain graphs using graph alignment. J. Neurosci. Methods 348, 109014.
Ying, R., You, J., Morris, C., Ren, X., Hamilton, W.L., Leskovec, J., 2019. Hierarchical graph representation learning with differentiable pooling. arXiv:1806.08804.
Zhang, X., Jian, W., Chen, Y., Yang, S., 2020. Deform-GAN: an unsupervised learning model for deformable registration. arXiv preprint arXiv:2002.11430.
Zheng, Y., Sui, X., Jiang, Y., Che, T., Zhang, S., Yang, J., Li, H., 2021. SymReg-GAN: symmetric image registration with generative adversarial networks. IEEE Trans. Pattern Anal. Mach. Intell. 44 (9), 5631–5646.
Zhou, J., Cui, G., Zhang, Z., Yang, C., Liu, Z., Sun, M., 2018. Graph neural networks: A review of methods and applications. CoRR abs/1812.08434. arXiv:1812.08434.